ELSEVIER

Journal of Structural Geology 29 (2007) 583–598

JOURNAL OF STRUCTURAL GEOLOGY

www.elsevier.com/locate/jsg

Deformation path partitioning within the transpressional White Mountain shear zone, California and Nevada

W.A. Sullivan [a,*], R.D. Law [b]

[a] *Department of Geology and Geophysics, Department 3006, University of Wyoming, 1000 University Avenue, Laramie, WY 82071, USA*
[b] *Department of Geosciences, Virginia Tech., Blacksburg, VA 24061, USA*

Received 15 June 2006; received in revised form 1 November 2006; accepted 2 November 2006
Available online 15 December 2006

Abstract

Most numerical simulations of transpression zones predict a change in finite stretching direction from subhorizontal to subvertical for simple shear-dominated zones. We provide a detailed description of a dextral transpression zone, the White Mountain shear zone (WMSZ), with a range of lineation orientations and compare these natural data to numerical models. The WMSZ is characterized by steeply dipping foliations, with dominant shallowly plunging lineations and coeval subordinate domains of steeply plunging lineations. Within shallowly lineated domains, foliation geometry, shear sense indicators and quartz *c*-axis fabrics indicate a large component of simple shear, while microstructural and quartz *c*-axis fabric data from steeply lineated domains indicate a large component of pure shear. Geometric relationships between foliations and lineations and quartz *c*-axis fabrics demonstrate that lineation orientation has remained constant during much of the deformation history. Comparison of numerical models with the data collected from WMSZ shows that the shear zone geometry and the observed strain path partitioning do not match any of these models. We propose a conceptual kinematic model for the WMSZ involving stable segregated coeval kinematic domains of simple shear-dominated fabrics and pure shear-dominated fabrics that accommodate the transcurrent and contractional components of deformation respectively.

Keywords: Strain path partitioning; Deformation partitioning; Transpression; White Mountain shear zone; White Mountains; Owens Valley

1. Introduction

The term transpression was first used by Harland (1971) to describe oblique convergence between tectonic plates, and it has since been recognized that many active plate boundaries are transpressive (e.g. Sumatra, central California and New Zealand) and that many exhumed orogenic belts contain geologic structures related to transpression (e.g. southern Appalachians, North American Cordillera and Scottish Caledonides) (Holdsworth et al., 1998 and references therein). Subsequently, Sanderson and Marchini (1984) used the term transpression to describe homogeneous deformation zones with orthogonal simple shear and pure shear components that accommodate both transcurrent and contractional deformation at transpressional plate boundaries. Sanderson and Marchini (1984) described this specialized case of transpressional deformation mathematically, producing a numerical model in which material is extruded freely in the vertical direction in response to the pure shear accommodated contractional component of deformation, while the transcurrent component of deformation is accommodated by progressive simple shear across the zone. Such a model predicts a consistent sense of fabric asymmetry, or shear sense indicators, on the horizontal exposure plane coupled with either a vertical maximum finite stretching direction or, for low angles of convergence, a switch in the maximum finite stretching direction from horizontal to vertical at some finite strain magnitude.

In the two decades since the introduction of the Sanderson and Marchini (1984) model, numerous workers have modified

* Corresponding author. Tel.: +1 307 760 5109; fax: +1 307 766 2697.
E-mail address: wasulliv@uwyo.edu (W.A. Sullivan).

0191-8141/$ - see front matter © 2006 Elsevier Ltd. All rights reserved.
doi:10.1016/j.jsg.2006.11.001

this basic model or produced numerical simulations of their own, and there exists in the literature an extensive body of work dealing with numerical simulation of transpression zones (e.g. Fossen and Tikoff, 1993; Tikoff and Teyssier, 1994; Robin and Cruden, 1994; Jones and Tanner, 1995; Dutton, 1997; Jones et al., 1997, 2004; Jiang and Williams, 1998; Jones and Holdsworth, 1998; Lin et al., 1998). All of these numerical simulations involve steady state deformation with incremental strains consisting of homogeneously distributed coeval simple shear and pure shear components in various combinations, and each of these models predict a different strain path and resulting finite strain geometries. The architects of most of these transpression models have compared their models to natural deformation zones and shown, with varying degrees of success, that the models can explain at least some strain features found within natural deformation zones (Robin and Cruden, 1994; Tikoff and Teyssier, 1994; Jones and Tanner, 1995; Dutton, 1997; Jones et al., 1997, 2004; Lin et al., 1998). A key element of all these numerical models (which combine pure and simple shear strain components of different orientations) is that while the orientation of the finite stretching direction changes with increasing strain magnitude due to the different rates at which strain accumulates under pure and simple shear, the externally imposed kinematic framework remains constant during progressive deformation.

Subsequently, several authors have invoked these models to explain fabric variations in steeply dipping high strain zones. For instance, Green and Schweickert (1995) used the Sanderson and Marchini (1984) model to explain variation in lineation orientation in the transpressional Gem Lake shear zone of eastern California, while Tikoff and Greene (1997) built on a refined version of the Sanderson and Marchini (1984) model published by Fossen and Tikoff (1993) to explain along strike variations in lineation orientation within the Sierra Crest shear system. Chetty and Bhaskar Rao (1998) also used the Fossen and Tikoff (1993) model to explain steeply plunging lineations within the Cauvery shear system, and Giorgis et al. (2005) used the Fossen and Tikoff (1993) model to explain steeply plunging lineations within the western Idaho shear zone. These studies have primarily used the numerical simulations of transpression zones to explain fabric variations within high strain zones, and few detailed critical comparisons between the predictions made by these numerical simulations and well-studied natural transpression zones have been made (see, however, Czeck and Hudleston, 2003).

In this paper we combine detailed field, microstructural and quartz *c*-axis fabric data in order to provide an in-depth analysis of a Late Cretaceous transpression zone, the White Mountain shear zone (WMSZ) exposed in eastern California and western Nevada. We then compare these data with predictions made by numerical simulations of transpression zones. In so doing, we show that the WMSZ is a dextral transpressional structure in which the transcurrent component of deformation is segregated from the contractional component of deformation, dividing the zone into discrete coeval segregated kinematic domains of simple shear-dominated and pure shear-dominated deformation. We propose a conceptual kinematic model in which the simple shear-dominated domains form an anastomosing network surrounding coeval segregated pure shear-dominated domains.

These data and interpretations are fundamentally incompatible with existing numerical simulations of transpression zones. In the WMSZ, the components of deformation, while stable in individual domains, are not evenly distributed throughout the deformation zone. We argue that the potential for strain path partitioning should be evaluated before applying numerical simulations of transpression zones based solely on fabric geometry (orientations of foliations and lineations).

2. Geologic setting of the White Mountain shear zone

2.1. White-Inyo Range

The White-Inyo Range in eastern California and western Nevada is the western-most crustal block in the central Basin and Range Province, and is situated on the inboard margin of the Sierran magmatic arc (Fig. 1). Geologic structures exposed

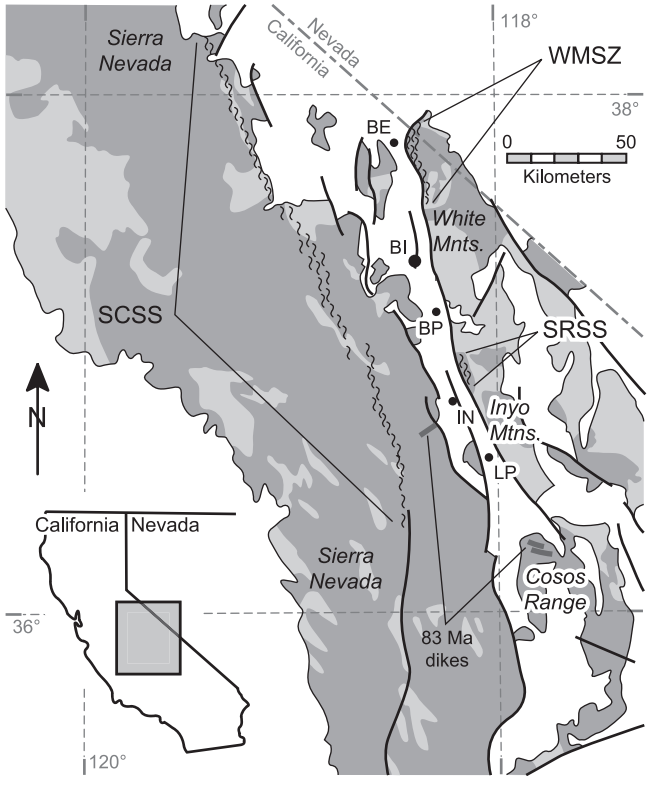

Fig. 1. Map showing locations of the White Mountain shear zone (WMSZ), Sierra Crest shear system (SCSS), and Santa Rita shear system (SRSS) in California and Nevada. Dark gray color represents Mesozoic plutonic rocks. Light gray color represents metamorphic and sedimentary rocks intruded by Mesozoic plutons. Light squiggly lines represent Late Cretaceous plastic shear zones. Heavy black lines represent Cenozoic strike-slip and normal faults. Abbreviations for towns are: BE, Benton; BI, Bishop; BP, Big Pine; IN, Independence; LP, Lone Pine. Compiled from USGS Map I-512, Crowder et al. (1972), Crowder and Sheridan (1972), Tikoff and Saint Blanquat (1997), Vines (1999), Lee et al. (2001) and Kylander-Clark et al. (2005).

in the central White-Inyo Range record a complex deformation history beginning with the Carboniferous Antler Orogeny (Stevens et al., 1997 and references therein) and include multiple episodes of Permian and Triassic contractional and extensional deformation (Stevens et al., 1997; Morgan and Law, 1998). During the Mesozoic, subduction along the western margin of North America was associated with formation of a continental magmatic arc, the Sierra Nevada Batholith, in addition to contractional and transpressional structures found both along the axis of the magmatic arc and behind the arc further inboard of the continental margin (Green and Schweickert, 1995; Stevens et al., 1997 and references therein; Tikoff and Greene, 1997; Tikoff and Saint Blanquat, 1997). In the central and southern White-Inyo Range, Late Jurassic to Early Cretaceous? contractional deformation is characterized by NE-directed reverse faulting, folding and cleavage development with a local sub-vertical stretching lineation, and this deformation is associated with a greenschist facies regional metamorphic event (Morgan and Law, 1998; Coleman et al., 2003).

Vines (1999) has described a dextral transpression zone, the Santa Rita shear system (SRSS), of probable Late Cretaceous age that crops out along the western flank of the southern White-Inyo Range along strike from the WMSZ (Fig. 1). Syn-deformational white mica, which only occurs within the SRSS and not in the wall rocks, has been dated at 83 Ma (^{40}Ar/^{39}Ar method; Bill McIntosh, New Mexico Geochronology Laboratory, personal communication, 2002). Because the SRSS and the WMSZ are roughly the same age, are kinematically similar and lie along strike from one another, we propose that they are part of a composite Late Cretaceous dextral transpressional shear zone system. The recognition of this composite SRSS–WMSZ system extends the known extent of Late Cretaceous dextral transpression eastward from the Sierra magmatic arc into the White-Inyo Range (Fig. 1).

We currently have no information on the amount of lateral motion on the SRSS–WMSZ system due to the lack of off-set markers and later normal faulting that resulted in burial of parts of the fault system beneath the Cenozoic sediments and volcanics of Owens Valley. However, ~65 km of N–S dextral off-set between the Sierra Nevada and the White-Inyo Range is indicated by correlating Devonian submarine channels and Permo-Triassic structures across the Owens Valley (Stevens et al., 1997, 2003; Stevens and Stone, 2002), and correlation of 83 Ma dikes exposed in the Sierra Nevada and in the Coso Range to the south of the Inyo Range (Fig. 1), indicates that 65 km of dextral slip has occurred since 83 Ma (Kylander-Clark et al., 2005). Additionally, based on correlation of elements of the ca. 148 Ma Independence dike swarm, Bartley et al. (in press) have shown that there has been as much as 130 km of dextral offset across the Owens Valley since 148 Ma, and they postulate that at least part of this offset is related to the SRSS–WMSZ system. Neogene dextral displacement across Owens Valley is probably no more than ~10 km (Lee et al., 2001), suggesting that appreciable dextral slip may have occurred in Late Cretaceous to Tertiary times (see also Glazner et al., 2005).

2.2. Northern White Mountains

The regional extent of the WMSZ was demarcated by U.S.G.S. quadrangle mapping in the 1960s and 1970s (Fig. 2a) (Crowder and Sheridan, 1972; Crowder et al., 1972). In the north, the WMSZ primarily deforms the ca. 90 Ma Pellisier Flats pluton and the marble and schist units lying along the western front of the range (Crowder et al., 1972). Near the southern end of the zone, the deformation fabric cuts Mesozoic metavolcanic and metasedimentary units (Crowder and Sheridan, 1972).

The bedrock geology of the northern White Mountains is dominated by two Late Cretaceous plutons, the Pellisier Flats biotite hornblende granite/quartz monzonite and the Boundary Peak biotite granite, with the Boundary Peak pluton being hosted almost entirely within the Pellisier Flats pluton (Fig. 2a) (Crowder et al., 1972; Crowder and Ross, 1973). The Pellisier Flats pluton has been dated at 91.7 ± 0.7 Ma (^{40}Ar/^{39}Ar, hornblende) and 88.0 ± 2.7 Ma (K–Ar, hornblende) by McKee and Conrad (1996), 89.6 Ma (U–Pb, zircon) by Stern et al. (1981) and 92.3 ± 3.0 Ma (K–Ar, hornblende) by Crowder et al. (1973). The Boundary Peak pluton has been dated at 71.7 ± 0.7 Ma (^{40}Ar/^{39}Ar, biotite) and 72.9 ± 2.5 Ma (K–Ar, biotite) by McKee and Conrad (1996) and 73.7 ± 2.2 Ma (K–Ar, biotite) by Crowder et al. (1973). For the purposes of this paper, we adopt an emplacement age of ~90 Ma for the Pellisier Flats pluton and recognize biotite cooling ages of ~73 Ma for the Boundary Peak pluton.

Along the western edge of the northern White Mountains, the Pellisier Flats pluton is partially mantled by marble layers and lesser amounts of schist and quartzite of probable Paleozoic? protolith age (Fig. 2a,b) (Crowder and Sheridan, 1972; Crowder et al., 1972). Marble units make up the bulk of the metasedimentary rocks in the northern White Mountains, and have locally been altered to skarns with the assemblage quartz + calcite + clinopyroxene + garnet + zoesite + opaque phase(s) + chlorite (retrograde). Elsewhere, marbles are nearly pure calcite with only minor quartz and tremolite. Schists range in composition from biotite + quartz + plagioclase feldspar + muscovite + opaque phase(s) ± andalusite in the central part of the field area to quartz + actinolite + clinozoesite + chlorite + graphite ± biotite near the southern end of the field area. Peak metamorphism in these rocks is inferred to be associated with Late Cretaceous contact metamorphism resulting from emplacement of the Pellisier Flats and Boundary Peak plutons. Exposures of these Paleozoic? metasedimentary rocks are almost entirely within the WMSZ, and no pre-shear zone fabric elements have been recognized in them.

South and east of the Pellisier Flats pluton there are extensive exposures of greenschist facies metavolcanic and metasedimentary rocks of Triassic and Jurassic protolith age (Fig. 2a) (Crowder and Sheridan, 1972; Fates, 1985; Hanson, 1986). An ash-flow tuff from the metavolcanic section has yielded an U–Pb zircon age of 152 + 5/−1 Ma (Hanson, 1986). Hanson (1986) recognized three distinct deformation events (D_1, D_2 and D_3) within the Triassic and Jurassic metavolcanic and

metasedimentary rocks of the northern White Mountains near the southern terminus of the mapped extent of the WMSZ (Fig. 2a). Hanson's, (1986) D_1 is characterized by a ~N–S-striking foliation, a shallowly to steeply plunging SW-trending lineation and small tight to isoclinal folds with axial planes roughly parallel to the D_1 foliation. D_1 fabrics and folds are most strongly developed within the WMSZ, but are not observed in the Late Cretaceous Pellisier Flats pluton. Hanson's, (1986) D_2 is characterized by N–S-trending west-vergent folds and thrust faults that apparently deform D_1 fabrics and folds outside of the WMSZ, but are poorly developed within, or structurally isolated from, the WMSZ. Finally, Hanson's, (1986) D_3 is characterized by E–W-trending crenulation, kink and/or large broad folds that are recognized throughout the Triassic and Jurassic metavolcanic/metasedimentary section. Additionally, Hanson (1986) recorded N–S-striking foliations and shallowly plunging N–S-trending lineations that are most strongly developed within the WMSZ and are associated with dextral S–C structures observed in the Pellisier Flats pluton. Based on these observations from the extreme southern end of the WMSZ, Hanson (1986) proposed two episodes of deformation for the WMSZ: (1) east-directed reverse faulting associated with the D_1 fabrics and folds that predates emplacement of the Pellisier Flats pluton, and (2) N–S-oriented dextral strike-slip movement associated with the apparently younger D_3 fabrics and S–C structures that postdate emplacement of the Pellisier Flats pluton. However, we argue, based on evidence presented below, that steeply plunging lineations and shallowly plunging lineations within the area examined for this study are coeval and represent one phase of deformation.

2.3. Cenozoic extensional faulting and block rotation

Many areas within the Basin and Range Province, including the White-Inyo Range, consist of relatively intact footwall blocks, bound on one side by range-scale high angle normal fault systems (e.g., Stewart, 1980). Much of the White-Inyo Range is bound on the west by the steeply west-dipping White Mountains and Inyo Mountains brittle fault zones (Fig. 1) which are Late Miocene to early Pliocene in age and accommodate as much as 8–9 km of normal sense displacement (Stockli et al., 2000, 2003). Detailed mapping of Oligocene and Early Miocene volcanic and volcaniclastic rocks deposited unconformably on Mesozoic and older plutonic and metamorphic rocks along the eastern margin of the White-Inyo Range indicates that faulting associated with Basin and Range tectonism has rotated the northern part of the range ~25° clockwise (i.e. down to the east) about a horizontal axis trending ~355° (Stockli et al., 2003).

3. Age of the White Mountain shear zone

Crowder et al. (1972) noted that the ca. 90 Ma Pellisier Flats pluton contains a strong solid state deformation fabric while the Boundary Peak pluton contains a weak fabric near its margins that appears to be related to deformation along the WMSZ, and consequently proposed that deformation along the WMSZ post-dates crystallization of the Pellisier Flats pluton and was waning at the time of emplacement of the Boundary Peak pluton. Sullivan (2003) has argued that deformation along the WMSZ must have continued for some time after emplacement of the Boundary Peak pluton. This assertion is based on the observations that: (1) deformation temperatures increase from ~400 °C to ~550 °C near the margins of the Boundary Peak pluton, (2) quartz *c*-axis fabric geometry undergoes gross temperature induced changes (requiring large amounts of strain) near the margins of the Boundary Peak pluton, and (3) deformed quartz within 400 m of the margins of the Boundary Peak pluton has undergone no static annealing recrystallization. However, deformation temperatures estimated from quartz *c*-axis fabrics collected from within 400 m of the margin of the Boundary Peak pluton (Sullivan, 2003) are well above the ~300 °C closure temperature for the K–Ar and $^{40}Ar/^{39}Ar$ systems in biotite indicating that deformation likely ceased before the ca. 73 Ma biotite cooling ages for the Boundary Peak pluton were reached.

Consequently, the age of the WMSZ can be bracketed at between ~90 and ~73 Ma, and a significant amount of strain must have developed after emplacement of the Boundary Peak pluton, but before cooling through ~300 °C. These ages closely agree with those for the dextral transpressional Sierra Crest and Santa Rita shear systems located to the west and south of the WMSZ (Fig. 1) (Green and Schweickert, 1995; Tikoff and Greene, 1997; Tikoff and Saint Blanquat, 1997; Vines, 1999), and place the WMSZ into a well established Late Cretaceous dextral transpressional plate tectonic setting.

4. Geometry of the White Mountain shear zone

4.1. Data collection

This study was restricted to the northern two-thirds of the WMSZ in the area that was not mapped by Hanson (1986). Due to the size of the area (~21.5 × 2 km) and the extremely rugged nature of the topography, detailed field mapping of the WMSZ is impractical. Therefore, field data was primarily collected in a series of 11 detailed traverses oriented at near right angles to the shear zone margins. These traverses are delineated by the location of structural data on the shear

Fig. 2. Geologic maps and field data. (a) Geologic map of the northern White Mountains showing the location of the WMSZ and the area mapped by Hanson (1986). (b) Map of the field area for this study showing generalized foliation form-lines, orientation of foliation and lineation data from four traverses across the shear zone, locations where transcurrent shear sense was observed in outcrop, locations of steeply lineated domains and sample localities discussed in the text. (c) Foliation and lineation orientation data from steeply lineated domains within the northern two-thirds of the WMSZ. (d) Detailed map of the area around two steeply lineated domains exposed in Montgomery Canyon. Lithologic contacts adapted or modified from Crowder et al. (1972), Crowder and Sheridan (1972) and Crowder and Ross (1973); foliation form lines indicate approximate map distribution of penetrative deformation associated with the WMSZ.

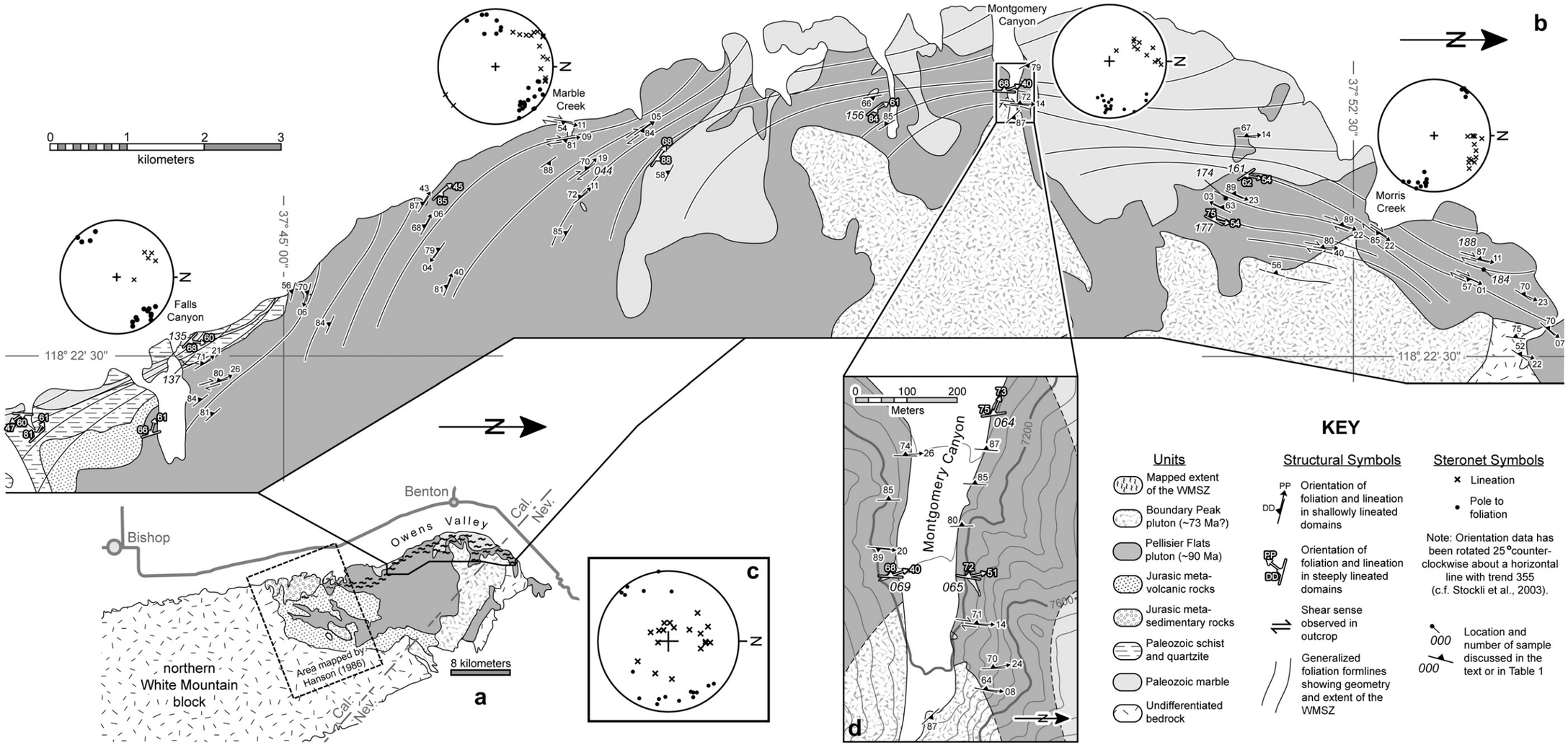
Marble Creek
Montgomery Canyon
Morris Creek
Falls Canyon
Montgomery Canyon
0 1 2 3
kilometers
0 100 200
Meters
— 37° 45' 00" —
— 37° 52' 30" —
118° 22' 30"
118° 22' 30"
N
b
c
d
a
Benton
Bishop
Owens Valley
Cal.
Nev.
Area mapped by Hanson (1986)
northern White Mountain block
8 kilometers
7200
7600
KEY
Units
Mapped extent of the WMSZ
Boundary Peak pluton (~73 Ma?)
Pellisier Flats pluton (~90 Ma)
Jurasic meta-volcanic rocks
Jurasic meta-sedimentary rocks
Paleozoic schist and quartzite
Paleozoic marble
Undifferentiated bedrock
Structural Symbols
Orientation of foliation and lineation in shallowly lineated domains
Orientation of foliation and lineation in steeply lineated domains
Shear sense observed in outcrop
Generalized foliation formlines showing geometry and extent of the WMSZ
Steronet Symbols
Lineation
Pole to foliation
Note: Orientation data has been rotated 25°counter-clockwise about a horizontal line with trend 355 (c.f. Stockli et al., 2003).
Location and number of sample discussed in the text or in Table 1

zone map in Fig. 2b. Full details of field data available for the northern part of the WMSZ can be found in Sullivan (2003). Emphasis was placed on mapping orientation of foliations and lineations within the mylonitic fabric, and on documenting variations in fabric intensity. Relative finite strains were estimated visually in the field based on deformation fabric intensity, or how well developed foliations and lineations are in a given outcrop relative to outcrops of similar rock types observed elsewhere in the WMSZ. 122 oriented samples were collected during field mapping and were cut perpendicular to foliation and both parallel and perpendicular to the mineral lineation for hand-sample based kinematic analyses. Thin sections were prepared from 50 of these samples for additional microstructure-based kinematic analyses.

As mentioned above, the northern end of the White Mountain crustal block, including deformation fabrics within the WMSZ, has been rotated by Cenozoic Basin and Range extensional faulting. To correct for Cenozoic tilting associated with Basin and Range tectonism, all of the structural orientation data presented in this paper from Cretaceous age structures have been rotated 25° counterclockwise (i.e. down to the west) about a horizontal axis trending towards 355° (cf. Stockli et al., 2003).

4.2. Description of deformation fabrics

The WMSZ is marked by a penetrative foliation and associated mineral lineation. We interpret mineral lineations within the WMSZ as true stretching lineations oriented parallel to the principal extension direction based on geometric relationships between lineations and quartz *c*-axis fabrics outlined in Section 5.3. Deformation fabric intensities are generally homogeneous at the outcrop scale. Within quartzites and schists, the foliation is defined by aligned chlorite, biotite and muscovite, and the mineral lineation in both quartzites and schists is defined by streaking of mica domains on foliation surfaces and in quartzites by quartz grain-shape alignment. Foliations and lineations in marbles are defined by a calcite grain-shape fabric and alignment of magnesium silicates. Lineation orientation across marble, schist and quartzite contacts seems to remain constant.

Foliation in the Pellisier Flats pluton is defined by: (1) an alignment of biotite, hornblende, metamorphic chlorite and local fine-grained metamorphic white mica, (2) ribboned quartz grains, and (3) alignment of long axes of feldspar grains. In localities with more intense deformation fabrics, the foliation is further defined by mechanically disaggregated feldspars and fine-grained metamorphic white mica. Feldspar grains have also undergone minor subgrain rotation dynamic recrystallization in the higher temperature parts of the WMSZ. The mineral lineation in these rocks is defined by streaking on quartz ribbons, streaking of mica domains and alignment of feldspar and hornblende crystals. In intensely deformed rocks lineations are further defined by trains of disaggregated feldspar grains. In S–C mylonites derived from the Pellisier Flats pluton C-surfaces are defined by planar domains of biotite, chlorite, fine-grained white mica and quartz ribbons, and S-surfaces are similar to foliations described above. Mineral lineations on C-surfaces are defined by a combination of: (1) streaking of mica domains, (2) ridge-and-groove style slicken lines in mica domains (Lin et al., 1992), and (3) streaking in quartz ribbons. S-surfaces in S–C mylonites were difficult to observe in the field. However, no orthogonal lineations were observed on S and C surfaces in S–C mylonites [*sensu* geometries proposed by Tikoff and Greene (1997) and Goodwin and Tikoff (2002) for grain-scale deformation path partitioning in S–C mylonites]. Complete transposition of S-surfaces into C-surfaces was not observed in the WMSZ, and the most intensely deformed rocks in shallowly lineated domains within the Pellisier Flats pluton are typically S–C mylonites. Where the Pellisier Flats pluton is in contact with meta-sedimentary rocks, it is generally weakly deformed or even undeformed, indicating that strain was partitioned into the meta-sedimentary rocks.

4.3. Shear zone geometry

At its northern end, in the Morris Creek area, the WMSZ is represented by a NE to NNE-striking foliation and shallowly to moderately plunging N to NNE-trending stretching lineations (Fig. 2b). The rocks exhibiting the most intense deformation fabrics and most clearly defined S–C relationships are located along the range front. Traced eastward, towards the shear zone margins in the Morris Creek area (Fig. 2b) the strike of foliation progressively changes from ~035° in the intensely deformed rocks to ~020–015° closer to the shear zone margins and S–C relationships can no longer be recognized. The dip of foliation also changes from vertical near the range front to steep-to-the-W closer to the shear zone margins.

In the area south of Morris Creek and in the Montgomery Canyon area (Fig. 2b,d), foliation within the WMSZ strikes ~N–S and dips steeply to the west. Stretching lineations in this area are north trending and vary from sub-horizontal to steeply plunging (Fig. 2b,d). S–C relationships were only observed in a few locations in this area, although the deformation fabric is locally strong in both shallowly and steeply lineated domains.

In the Marble Creek area (Fig. 2b), foliation within the WMSZ strikes ~N–S near the range front, where the most intense deformation fabrics and most clearly defined S–C relationships are found, and swings to the NW to WNW near the margins of the shear zone to the east where only S-surfaces are present. Traced eastward, the dip of foliation changes from steep-to-the-E at the range front to near-vertical to steep-to-the-W as the strike of foliation swings around to the NW and the deformation fabric weakens. Stretching lineations in the Marble Creek area trend N to NW and are shallowly plunging (Fig. 2b).

At the southern end of the study area, near Falls Canyon (Fig. 2b), the WMSZ primarily cuts meta-sedimentary rocks and is characterized by a NW to NNW-striking steeply W-dipping to near-vertical foliation and NNW-trending shallowly to steeply plunging stretching lineations (Fig. 2b). In the Falls

Canyon area, the most intense deformation fabrics are found in the marbles, schists and quartzites located along the range front, whereas deformation fabrics within the Pellisier flats pluton are generally weaker and quite heterogeneous and in some outcrops there is no observable fabric. The metasedimentary rocks in this area contain both steeply lineated and shallowly lineated domains, whereas lineations measured in the Pellisier Flats pluton are shallowly plunging.

To summarize, the strike of the near-vertical foliation within the northern two-thirds of the WMSZ varies from NNE in the extreme northern end of the range to NNW near the southern end of the study area, and the strike of foliation tends to swing towards the west near the shear zone margins (Fig. 2b). The observed foliation map pattern is similar to that expected for a N–S trending subvertical transcurrent simple shear zone (*sensu* Ramsay and Graham, 1970), but in which the foliation in the center of the zone is a C-surface and the west half of the shear zone has been removed by normal faulting. Stretching lineations within the WMSZ are predominantly subhorizontal to shallowly N-plunging, and subordinate domains of steeply plunging stretching lineations are present throughout much of the WMSZ.

4.4. Variations in lineation orientation

Stretching lineations within the WMSZ are generally subhorizontal to moderately north-plunging. However, interspersed throughout the WMSZ there are discrete localized domains of steeply plunging (pitch on foliation of 45° or more) stretching lineations. Like the shallow lineations, the steeply plunging lineations generally trend towards the north, and the orientation of foliation in these domains parallels that found in nearby shallowly lineated mylonites (Fig. 2b–d). These domains are found within both the Pellisier Flats pluton and the older Paleozoic? metasedimentary rocks, but are not found in S–C mylonites. Through examination of successive foliation planes across strike, steeply plunging lineations can locally be continuously traced into shallowly plunging lineations within a single outcrop and no overprinting fabrics were observed either in the Pellisier Flats pluton or the older units. These relationships indicate that steeply plunging and shallowly plunging lineations within the WMSZ formed contemporaneously, rather than during two separate deformation events as proposed by Hanson (1986).

Traced across strike, steeply lineated domains vary in width from a few tens of meters to 200 m or more. We have not attempted to map the steeply lineated domains between transects, but, within the resolution of our map data, there does not appear to be any regular map pattern distribution of these domains. A transect map showing two steeply lineated domains is presented in Fig. 2d. Microstructural and quartz *c*-axis fabric data from these domains are presented in Table 1 and Fig. 4e,f. The Paleozoic? marble in the Montgomery Canyon area (Fig. 2d) is poorly exposed and is generally too brecciated to provide useful structural data. Near the contact with the marble, the Pellisier Flats pluton is only weakly deformed, and foliation surfaces were not observed in outcrop; hence, no lineation data is reported for some field stations.

Steeply lineated domains can be found in both relatively high strain and relatively low strain (estimated from

Table 1
Summary of sample orientations and kinematic data collected from oriented thin sections where the pitch of the stretching lineation on the foliation was greater than 45°, location of samples is indicated in Fig. 2b

Sample no.	Lithology	Orientation of foliation	Orientation of lineation	Pitch of lineation	Microstructure based shear sense indication	Flow type	Movement direction in geographic coordinates	Quartz *c*-axis fabric geometry and Fig. number	Relative finite strain magnitude
064	Pellisier Flats	350/75-W	292-73	81	None	Pure shear	N/A	Not measurable	Medium
065	Quartzose skarn	009/72-W	347-51	54	Weak type-II S–C	General shear	Oblique dextral/top-to-W normal-sense	Symmetric X-girdle, Fig. 4e	High
069	Quartzose skarn	003/68-W	340-40	49	None	Pure shear	N/A	Symmetric X-girdle, Fig. 4f	High
135	Marble	317/79-E	112-49	53	None	Pure shear	N/A	Not applicable	High
137	Impure quartzite	336/68-W	316-42	45	Type-II S–C, Fig. 3d	General shear	Oblique dextral/top-to-W normal-sense	Symmetric X-girdle, Fig. 5c	Medium
156	Pellisier Flats	310/84-E	318-61	62	Shear bands	General shear	Oblique dextral/top-to-W reverse-sense	Not measurable	Medium
161	Pellisier Flats	329/62-E	013-54	64	None	Pure shear	N/A	Not measurable	Low
174	Pellisier Flats	050/61-N	023-40	48	None	Pure shear	N/A	Not measurable	High
177	Pellisier Flats	021/75-W	358-54	58	Weak shear bands	General shear	Oblique sinistral/top-to-E reverse-sense	Not Measurable	Low

N/A, not available.

deformation fabric intensity) portions of the WMSZ, indicating that there is little or no link between apparent finite strain magnitude and lineation orientation. Moreover, both shallowly and steeply lineated domains within the WMSZ are characterized by well developed L–S tectonites with sparse L > S and S > L tectonites (Flinn, 1965). Pure S-tectonites were not observed at any location in the field area. In some localities with a weak fabric, foliation planes and hence potential lineations could not be examined. These observations, coupled with quartz *c*-axis fabric data presented below, indicate that most domains within the WMSZ have not experienced the large components of flattening strain that are predicted by numerical simulations of transpression zones.

5. Kinematic analyses

5.1. Shallowly lineated domains

A strong degree of fabric asymmetry is associated with shallowly plunging lineations and is best observed on faces cut perpendicular to the foliation and parallel to the lineation. In the domains exhibiting a steeply dipping foliation and sub-horizontal stretching lineations the section planes are viewed looking vertically down into the ground. S–C fabrics (Berthé et al., 1979) yielding a dextral shear sense are often well developed within the Pellisier Flats pluton and are commonly observed in outcrop within the northern half of the WMSZ (Figs. 2b, 3c). The most spectacular examples of S–C fabrics are found at the extreme northern end of the shear zone in a coarse grained facies of the Pellisier Flats pluton exposed in the Morris Creek area where individual C-surfaces are separated by as much as 2 cm (Fig. 3c).

Shear sense indicators observed in thin-sections cut from sub-horizontally lineated samples are almost universally dextral. Type-I S–C fabrics (Berthé et al., 1979; Lister and Snoke, 1984) are commonly observed within sections cut from mylonites of the Pellisier Flats pluton and Type-II S–C fabrics (Fig. 3d,e) (Lister and Snoke, 1984) are common in deformed quarzites, quartz rich skarns and quartz veins. Asymmetric recrystallized pressure shadows and shear bands (Hanmer and Passchier, 1991) indicating a dextral shear sense are present in many of the sheared Paleozoic? marbles and schists. Single-girdle and asymmetric cross-girdle quartz *c*-axis fabrics (Lister, 1977; Lister and Hobbs, 1980; Law, 1990) also confirming a dextral shear sense have been recorded in shallowly lineated domains in the Morris Creek and Marble Creek areas (Figs. 4c,d, 5a). These asymmetric quartz *c*-axis fabrics indicate a relatively large component of simple shear within the shallowly lineated domains (Lister and Hobbs, 1980; Law, 1987, 1990).

An overall dextral transcurrent shear sense for the WMSZ is also indicated by the kilometer-scale foliation geometry. Traced eastwards in the Marble Creek area, the strike of foliation swings from ~N–S in the intensely deformed rocks near the range front to ~NW near the shear zone margins (Fig. 2b). Such a swing in the strike of subvertical foliation is similar to that expected for the east half of a N–S-striking ideal dextral transcurrent simple shear zone (Ramsay and Graham, 1970). This feature is also present in the Morris Creek area where the strike of foliation swings ~15–20° to the west between the intensely deformed rocks located along the range front and the eastern margin of the shear zone (Fig. 2b).

5.2. Steeply lineated domains

As outlined in section 4.2, domains of steeply plunging lineations (pitch on the foliation of 45° or more) were observed in several locations within the northern two-thirds of the WMSZ (Fig. 2b–d), and these domains appear to be coeval with the more prevalent shallowly plunging lineations. As with the shallowly lineated samples, cut faces and thin sections were examined both perpendicular and parallel to the lineation; little or no fabric asymmetry was observed on faces cut perpendicular to lineation within the steeply lineated domains. Additionally, no asymmetric fabrics were observed on sub-horizontal faces within steeply lineated domains examined in the field. This is in marked contrast to the shallowly lineated domains in which dextral S–C fabrics were readily visible on sub-horizontal faces within the Pellisier Flats pluton.

Microstructure-based kinematic data collected from domains within the WMSZ exhibiting stretching lineations with a pitch on the foliation of more than 45° are summarized in Table 1. Of the nine samples for which kinematic data are available, five exhibit no discernible sense of fabric asymmetry. That is, no composite foliations were recognized and the direction of rotation (if any) of rigid objects is ambiguous. These five samples span the complete range of relative deformation fabric intensities observed in the steeply lineated domains, and the lack of fabric asymmetry is attributed to a large component of pure shear. In geographic coordinates, two of the remaining samples yield an oblique dextral/top-down-to-the-west normal-sense motion, one yielded an oblique sinistral/top-up-to-the-east reverse-sense motion, and one yielded an oblique dextral/top-up-to-the-west reverse-sense motion (Table 1). In other words, no consistent sense of motion in geographic coordinates was observed in the steeply lineated domains. However, the foliation in the sample exhibiting a component of top-up-to-the-west reverse-sense movement (sample 156 in Table 1, Fig. 2b) dips at 84° to the east after the 25° counter-clockwise rotation used to correct for subsequent block rotation associated with Basin and Range faulting. If the block rotation correction were reduced by 9° or more, this sample would exhibit oblique dextral/top-down-to-the-west normal-sense motion; making a total of three of four samples with this sense of motion.

Nearly symmetrical cross-girdle quartz *c*-axis fabrics were collected from two of the high strain samples and one of the medium strain samples (Figs. 4d,e, 5c). Two of these *c*-axis fabrics (Fig. 4e,f) were collected from quartz rich skarns shown on Fig. 2d. These bodies also contain high-grade schist and have no large populations of rigid porphyroblasts. Based on their composition, we interpret them to be rheologically weaker than the surrounding plutonic rocks. Elsewhere

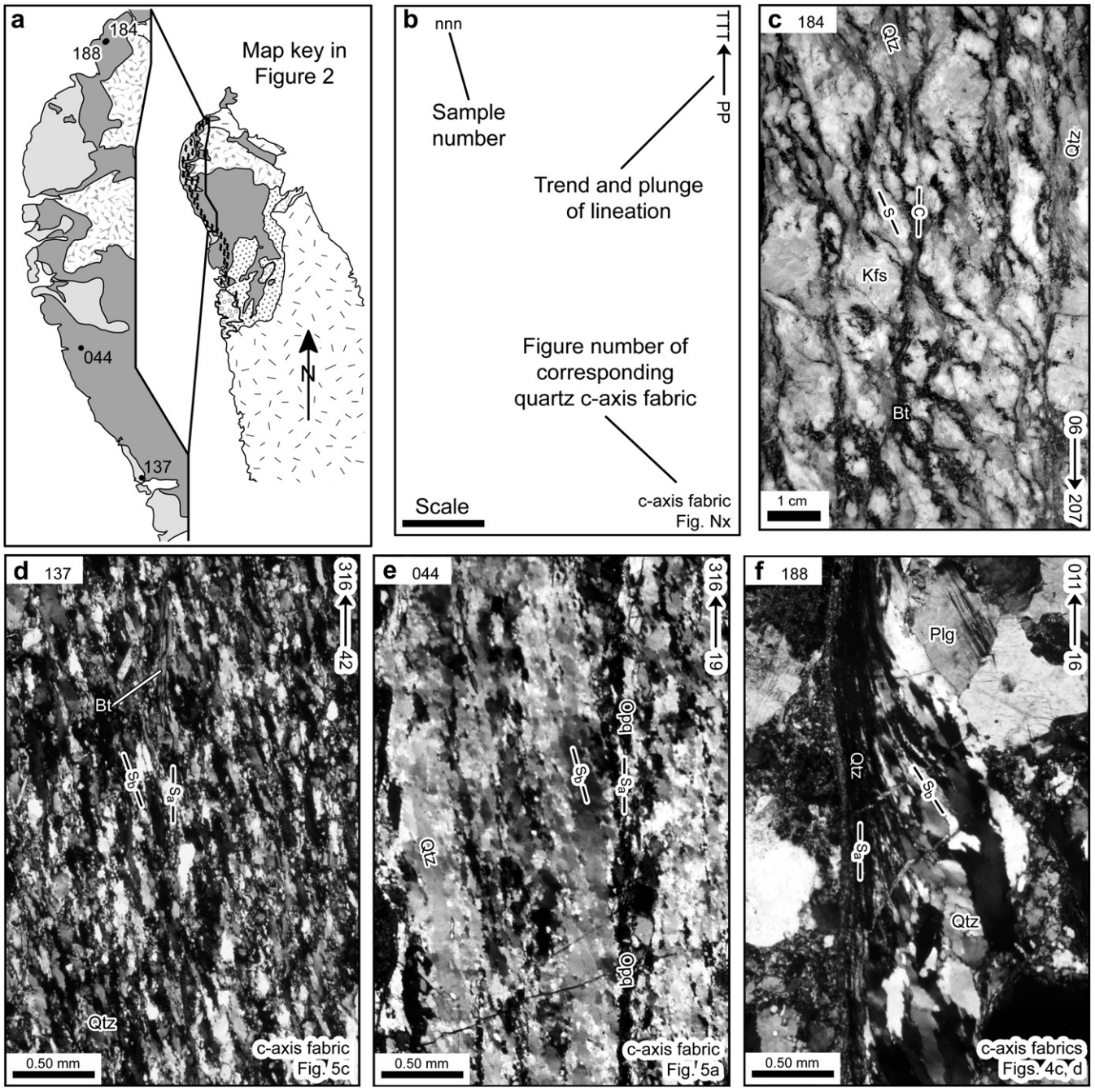

Fig. 3. Deformation fabrics from the northern two thirds of the WMSZ. Photographed faces are cut perpendicular to foliation and parallel to mineral lineation and viewed downwards. (a) Map showing locations from which samples (c–f) were taken. (b) Diagram explaining notation on photographs. (c) Type-I S–C fabrics on a cut face of mylonite of the Pellisier Flats pluton; sense of obliquity between spaced and penetrative foliation (C and S surfaces) indicates a dextral shear sense. (d) Type-II S–C mylonitic quartz vein; sense of obliquity between penetrative foliation (S_a) and oblique alignment (S_b) of elongate dynamically recrystallized quartz grains indicates a dextral shear sense. (e) Dextral type-II S–C mylonitic quartz vein from Marble Creek. (f) Dextral C (S_a)–S (S_b) relationships in ribboned quartz grain from mylonite of the Pellisier Flats pluton. Mineral abbreviations: Bt, biotite; Kfs, potasic feldspar; Opq, opaque minerals; Plg, plagioclase feldspar; Qtz, quartz.

symmetrical cross-girdle *c*-axis fabrics were collected from quartzite units (Fig. 5b–d) that are likely rheologically stronger than interbedded schist and marble domains. The presence of these symmetric *c*-axis fabrics supports the notion that the steeply lineated domains experienced a pure shear-dominated deformation (Lister and Hobbs, 1980; Law, 1990). Therefore, it seems that the domains of steeply plunging lineations within the WMSZ represent areas of pure shear-dominated fabrics within what, at a larger scale, is dominantly a dextral transcurrent simple shear zone. It should be noted that two of the samples from the shallowly lineated domains also yielded nearly symmetrical cross-girdle quartz *c*-axis fabrics (Fig. 5b,d). One of these samples has a lineation with a pitch on the foliation of 42° and

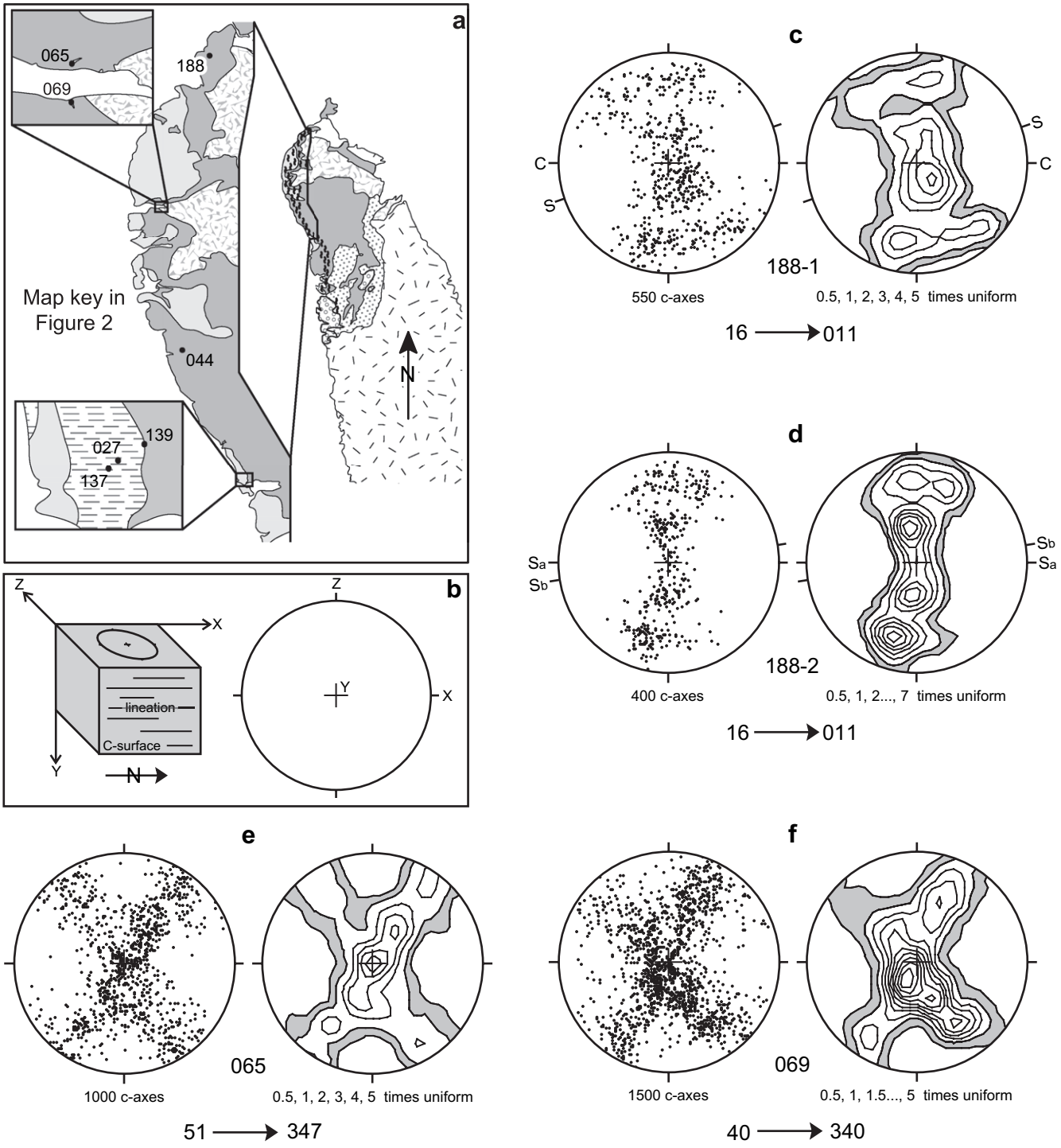

Fig. 4. Quartz *c*-axis fabrics from the northern part of the study area. Sample locations for the northern (Fig. 4) and southern (Fig. 5) parts of study area are given in (a). (b) Reference frame for all reported *c*-axis fabrics in Figs. 4 and 5; all projections are equal area lower hemisphere oriented perpendicular to the steeply dipping foliation (either C or composite C-S surface) and parallel to the stretching lineation. (c and d) fabrics from different ribboned quartz grains of the same sample of homogenously deformed Pellisier Flats granite, with (c) including ribbons from both the S and C surfaces and (d) being entirely from a single quartz ribbon within one C surface; a photomicrograph of this sample is presented in Fig. 3f. (e, f) Fabrics from quartz rich skarns that are now xenoliths hosted in the Pellisier Flats pluton. Orientations of S and C or penetrative foliation (S_a) and oblique alignment (S_b) of elongate dynamically recrystallized quartz grains have been marked for samples where these relations were observed. Sample numbers are given between the scatter and contour plots and the trend and plunge of the stretching lineation for each sample is given below the fabric plots.

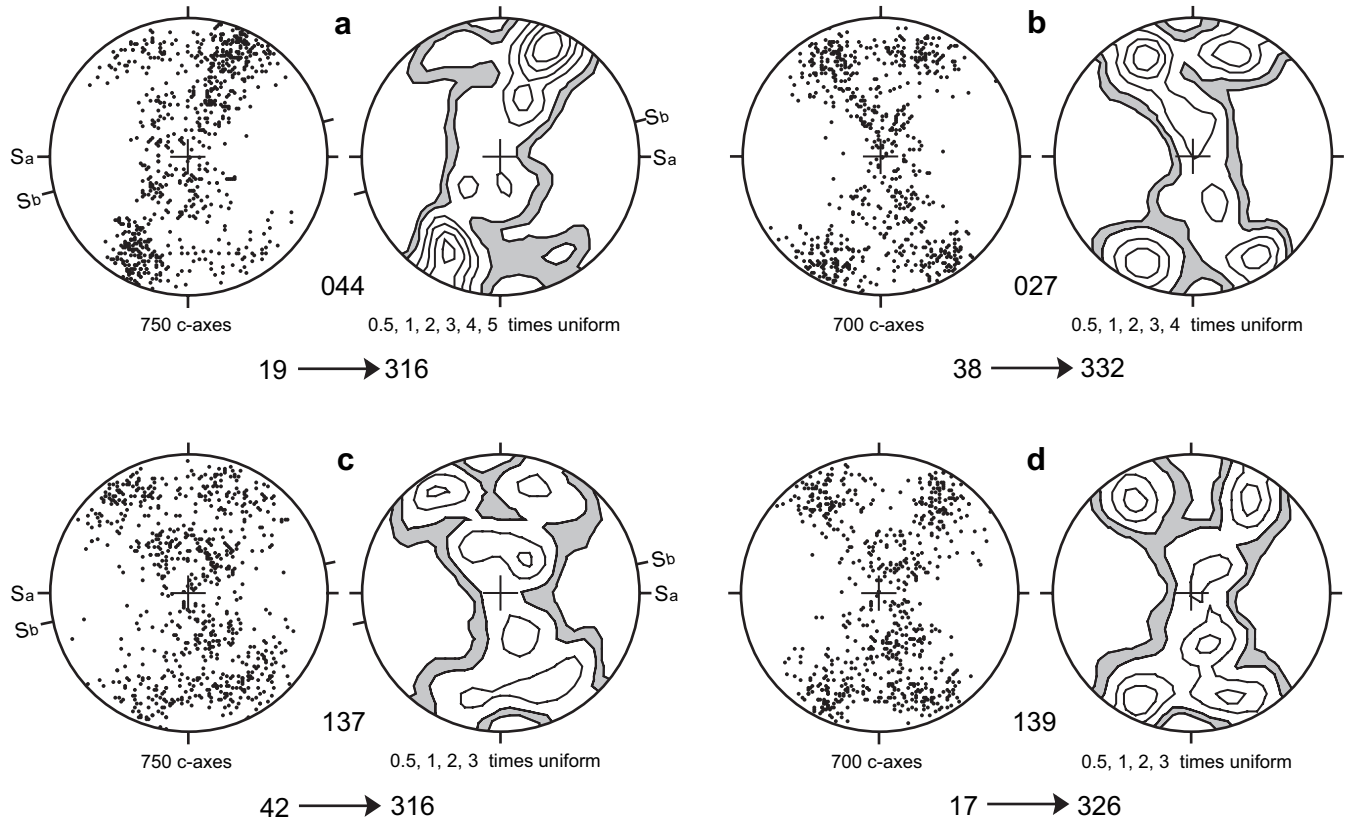

Fig. 5. Quartz *c*-axis fabrics form the southern part of the study area. Sample locations are given in Fig. 4a. (a) Fabric from a sheared quartz vein hosted within the Pellisier Flats pluton at Marble Creek; a photomicrograph of this sample is presented in Fig. 4e. (b–d) Fabrics from sheared impure quartzites hosted within schist at Falls Canyon; a photomicrograph of sample 137 is presented in Fig. 3d. All projections are equal area lower hemisphere oriented perpendicular to the steeply dipping foliation and parallel to the stretching lineation. Orientations of penetrative foliation (S_a) and oblique alignment (S_b) of elongate dynamically recrystallized quartz grains have been marked for samples where observed. Sample numbers are given between the scatter and contour plots and the trend and plunge of the stretching lineation is given below the fabric plots.

thus lies just outside of our steep lineation group. However, the other sample (Fig. 5d) is shallowly lineated, indicating that some of the shallowly lineated mylonites of the WMSZ must also have undergone pure shear-dominated deformation.

5.3. Kinematic framework and shape fabric stability

Numerical simulations of quartz crystallographic fabric formation indicate that crystallographic fabric pattern and orientation is controlled by the external kinematic framework (e.g. stress directions) imposed upon the deformed rock rather than by the magnitude of finite strain (Lister and Hobbs, 1980; Wenk et al., 1989; Jessell and Lister, 1990). These studies predict that the main girdle of the quartz *c*-axis fabric will form perpendicular to the flow plane in both strict pure and simple shear, and that the fabric pattern will only strengthen with increasing finite strain, not rotate with respect to the external kinematic framework (Lister and Hobbs, 1980; Jessell and Lister, 1990; Takeshita et al., 1999). These conclusions are strongly supported by many experimental simple shear and general shear deformation studies of quartz and analogue materials (e.g. Bouchez and Duval, 1982; Herwegh and Handy, 1996; Herwegh et al., 1997; Takeshita et al., 1999). Although, two recent experimental studies involving general shear in quartzite have produced quartz *c*-axis fabrics whose main girdle is oriented oblique to the flow plane and progressively rotates with increasing shear strain (Heilbronner and Tullis, 2002, 2006). In these recently reported general shear quartzite experiments (we estimate a pure shear component of 9–14% from the quoted shortening and shear strain data), Heilbronner and Tullis (2006) have documented a progressive transition from a *Z*-axis maxima to a *Y*-axis maxima (cf. Fig. 4b) with increasing strain-induced grain boundary migration recrystallization. This transition occurs because grains oriented favorably for prism <*a*> slip preferentially consume other grains during grain boundary migration recrystallization (regime III of Hirth and Tullis, 1992). This ultimately leads to a mechanical steady state and a stable *c*-axis fabric pattern dominated by a *Y*-axis maxima (Fig. 4b). In the experimentally deformed samples, a steady state was achieved at shear strains of ~8. However, because of the limitations imposed by the experimental conditions, these samples were deformed at the lower temperature/upper strain rate end of regime III dynamic recrystallization (e.g. some subgrain rotation recrystallization still visible). A steady state should be reached at lower strains in naturally deformed quartzites where grain boundary migration recrystallization can proceed at a much faster rate

(Jan Tullis, personal communication, 2006). No evidence exists for similar dynamic recrystallization-driven changes in *c*-axis fabric patterns collected from samples that are not characterized by regime III dynamic recrystallization. Because quartz *c*-axis fabrics collected from our samples characterized by regime III dynamic recrystallization (samples 188-1, 065 and 069 shown in Fig. 4c,e,d, respectively) have *Y*-axis maxima and skeletal patterns expected for the relatively high deformation temperatures indicated by the microstructures (Law, 1990; Hirth and Tullis, 1992; Heilbronner and Tullis, 2006), we feel that these samples have reached a steady state and can be used to make inferences about the geometry of the deformation imposed upon the samples.

From these arguments, it follows that the quartz *c*-axis fabrics collected from the WMSZ record the external kinematic framework (flow plane and direction for pure shear component and shear plane and direction for simple shear component) imposed on that particular sample. All quartz *c*-axis fabrics from both shallowly and steeply lineated samples from the WMSZ, measured on section planes oriented perpendicular to foliation and parallel to lineation (*XZ* planes), are characterized by well developed girdles (single or cross) oriented at a high angle to the foliation plane and centered about the *Y* (intermediate) finite strain axis (Figs. 4, 5, 6b,c). These geometric relationships indicate that regardless of angle of lineation plunge: (1) the mineral lineations are true stretching lineations, (2) these samples were deformed under approximate plane strain conditions (Tullis, 1977; Lister et al., 1978; Lister and Hobbs, 1980; Price, 1985; Law, 1986; Schmid and Casey, 1986), and (3) the orientation of stretching lineations within these samples has remained constant with respect to the crystallographic fabrics and hence the external kinematic framework imposed upon the samples.

Strictly speaking, quartz crystallographic fabrics record only the external kinematic framework and subsequent deformation history imposed on the volume of rock from which the fabric was measured. This gives rise to the possibility of deformation path partitioning between the quartz domains from which the quartz *c*-axis fabrics were measured and other domains of differing rheologies within the WMSZ, and some amount of deformation partitioning between different rheological domains has almost certainly occurred (Lister and Williams, 1983; Jiang, 1994a,b; Goodwin and Tikoff, 2002). Indeed, at the very least, rheologically weaker mineral phases and rock units have taken up more of the bulk strain. However, there is no observed variation in lineation orientation between different rheological domains (e.g. between S and C domains in the S–C mylonite or between lithologic units in the metasedimentary rocks) within the WMSZ, and the microstructural, hand sample and outcrop textural analyses of heterogeneous rocks generally agree with the kinematic framework and deformation geometries implied by the quartz *c*-axis fabrics. Furthermore, quartz *c*-axis fabrics collected from quartz ribbons contained in both S and C surfaces of the same sample indicate that there was no rotation of the kinematic axes between these two domains in at least the quartz ribbons (Fig. 4c,d). These observations argue that, though the quartz *c*-axis fabrics from a heterogeneous volume of rock from the WMSZ do not record the bulk deformation path of an entire sample or outcrop, they do record the overall geometry of the deformation.

Based on this reasoning and the quartz *c*-axis data, it seems that the domains of steeply plunging stretching

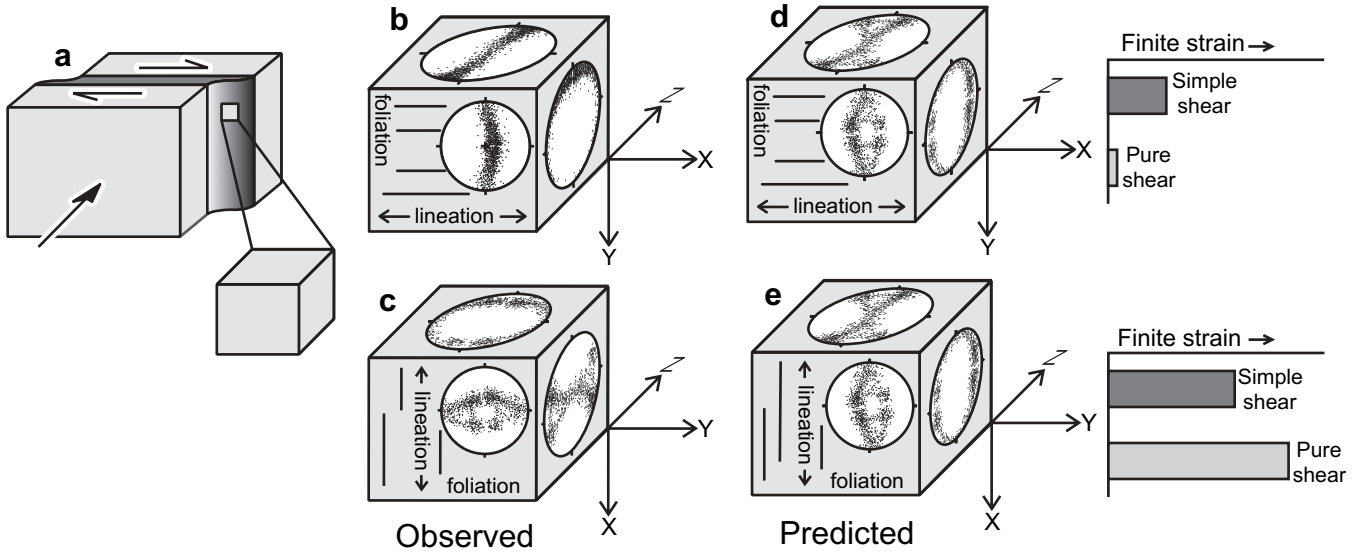

Fig. 6. (a) Schematic diagrams showing geometric relationships for a dextral transpressional shear zone. (b) Single girdle quartz *c*-axis fabric orientation (e.g. Fig. 4d) observed within shallowly lineated mylonites from the WMSZ. (c) Cross girdle quartz *c*-axis fabric orientation (e.g. Fig. 4e) observed within steeply lineated mylonites from the WMSZ. (d) Cross girdle quartz *c*-axis fabric orientation relative to shape fabric orientation predicted for low finite strains by numerical simulations of transpression zones; relative contributions of pure shear and simple shear components to finite strain are schematically illustrated. (e) Cross girdle quartz *c*-axis fabric orientation relative to shape fabric orientation predicted for high finite strains by numerical simulations of transpression zones that involve a change in orientation of the maximum finite stretching direction (but not externally imposed kinematic framework) with increasing strain magnitude.

lineations found within the northern half of the WMSZ must represent a kinematic framework that localizes relatively large components of pure shear and is separate from, but coeval with, the dominant dextral transcurrent framework of the WMSZ. In other words, the pure shear-dominated contractional deformation within the WMSZ is being partitioned into discrete domains that are kinematically distinct from the rest of the shear zone. This assertion could be tested by conducting kinematic vorticity analyses on both the steeply lineated domains and on the typical shallowly lineated portions of the WMSZ. However, the absence of finite strain markers and independently rotating rigid clasts within the WMSZ makes these rocks unsuitable for existing vorticity analysis techniques such as those proposed by Passchier (1988), Simpson and De Paor (1993, 1997) and Wallis (1992, 1995).

6. Discussion and application of transpression models

6.1. Comparison with numerical simulations of transpression zones

All of the currently available numerical models of transpression zones combine differently oriented components of pure shear and simple shear, and, for some modeled deformation regimes, this arrangement can lead to a switch (either progressive or instantaneous) in the maximum finite stretching direction due to the more efficient accumulation of strain under pure shear deformation (Sanderson and Marchini, 1984; Fossen and Tikoff, 1993; Robin and Cruden, 1994; Tikoff and Teyssier, 1994; Jones and Tanner, 1995; Dutton, 1997; Jones et al., 1997, 2004; Jiang and Williams, 1998; Jones and Holdsworth, 1998; Lin et al., 1998). Many of these models can then be used to explain variations in stretching lineation orientation like those outlined for the WMSZ. All of these models also make the fundamental assumption that the externally imposed kinematic framework remains constant throughout deformation. Therefore, because quartz crystallographic fabric patterns should remain in a constant orientation with respect to the external kinematic framework (but cf. experimental results of Heilbronner and Tullis, 2006) rather than the axes of the finite strain ellipsoid, these models predict that the orientation of quartz *c*-axis patterns developed under kinematic regimes similar to those of the model transpression zones should also remain in a constant orientation. In other words, if the plunge of the maximum finite stretching direction in such a transpression zone were to change, either instantaneously or progressively, one would expect to see a relationship between crystallographic fabric and shape fabric orientations similar to that depicted in Fig. 6d,e. In such a case, after reorientation of the shape fabric as predicted by numerical simulations, the main girdle of a quartz *c*-axis fabric that developed in response to the external transpressional kinematic framework would be oriented oblique to the lineation. Such a *c*-axis fabric viewed in the plane perpendicular to the foliation and parallel to the lineation would take on the appearance, or a hybrid of the appearance of, that depicted on the *XZ* section of Fig. 6e.

The Sanderson and Marchini (1984) transpression zone model, and those derived from it that utilize orthogonal pure and simple shear components (Fossen and Tikoff, 1993; Tikoff and Teyssier, 1994; Jones and Tanner, 1995; Jones et al., 1997), all predict stretching lineations that are subhorizontal, subvertical or both. Consequently, they are inadequate to explain the range of obliquely plunging stretching lineations found within the WMSZ (Fig. 2b–d). Numerical models of transpression zones that predict obliquely plunging stretching lineations similar to those described for the WMSZ include coupled boundary models (Robin and Cruden, 1994; Dutton, 1997) and triclinic transpression zone models (Jiang and Williams, 1998; Jones and Holdsworth, 1998; Lin et al., 1998; Jones et al., 2004). Both these groups of models are considered in turn below.

The coupled boundary models (Robin and Cruden, 1994; Dutton, 1997) predict that the pure shear component will be greatest near the edge of the deformation zone and that the most intense deformation fabrics will be in this region. Because of this, the strike of foliation will parallel the shear zone boundaries near the shear zone margins and be oblique to the shear zone boundaries in the center of the zone (Dutton, 1997). This pattern is opposite to that expected for the strike of foliation in an ideal simple shear zone (Ramsay and Graham, 1970). At the same time, this model predicts that foliation will dip away from the center of the zone near the shear zone margins and be vertical in the center of the zone (Dutton, 1997). Maximum lineation plunge should be achieved where the pure shear component is greatest, near the shear zone boundaries.

These predictions do not fit well with the observed foliation and lineation orientations from the WMSZ. First, the most intense deformation fabrics seem to be in the center of the shear zone and do not always correlate with the steeply plunging lineations. Second, although the dip of foliation does decrease near the margins of the WMSZ, the foliation dips towards rather than away from the center of the zone. Third, these models predict large amounts of flattening strain, and this is in marked disagreement with approximate plane strain symmetries indicated by both the observed shape fabrics (L–S tectonites) and the quartz *c*-axis fabrics collected from the WMSZ. Hence, it does not seem that the deformation fabrics within the WMSZ can be explained using the coupled boundary transpression zone models.

The triclinic transpression zone models (e.g. Jones and Holdsworth, 1998; Lin et al., 1998; Jones et al., 2004) also evolved from the basic geometry of the Sanderson and Marchini (1984) model, but the deformation components are oblique to one another. These models combine: (1) a pure shear component oriented with the intermediate stretching direction parallel to the strike of the zone and the maximum stretching direction in the vertical direction, perpendicular to the strike of the zone and, (2) a simple shear component of deformation wherein displacement is parallel to the zone margins but oblique to the maximum stretching direction of the pure shear component. The vorticity vector is considered to be perpendicular to the plane containing the simple shear component of

deformation, the vorticity normal section or VNS (Jiang and Williams, 1998; Jones and Holdsworth, 1998; Lin et al., 1998). For shear zones with relatively small components of pure shear, the lineation is initially located in the VNS, and as finite strain increases, the lineation is predicted to progressively rotate away from the VNS towards the vertical (Jiang and Williams, 1998; Jones and Holdsworth, 1998; Lin et al., 1998). This model also predicts that foliation will initially strike obliquely to the shear zone margins and dip steeply towards the center of the zone and that the foliation will progressively rotate into parallelism with the shear zone walls as finite strain increases. Like the coupled boundary condition models, the triclinic transpression zone models predict that the lineations with the steepest plunge will be located in the areas with the most intense deformation fabrics. Thus, for a N–S dextral transpression zone with a very high component of simple shear and the VNS (simple shear component) oriented at ~10–20° to the horizontal, this model predicts that the lineation will initially plunge at ~10–20° while the foliation will dip steeply to the east and strike at about 345°. The shape fabric patterns predicted by the Jones et al. (2004) inclined transpression zone model for a steeply west-dipping triclinic transpression zone with a small component of dip-slip motion (shallowly dipping VNS) are very similar to those predicted by the vertical triclinic transpression zone models.

At first glance, the triclinic model for a high simple shear/pure shear ratio and a VNS at about 10–20° to the horizontal provides a good fit for the observed foliation and lineation patterns from the shallowly lineated domains of the WMSZ. However, the steeply lineated domains within the WMSZ are not always found in conjunction with the most intense deformation fabrics as predicted by the triclinic transpression zone models. This discrepancy could be explained by having a heterogeneously distributed pure shear component of deformation causing some areas to have stretching lineations rotate towards the vertical at a much greater rate. Such an arrangement would be in close agreement with the observed partitioning of pure shear and simple shear components of deformation discussed in Sections 5.1 and 5.2. However, there are two important flaws with this arrangement: (1) some of the shallowly lineated domains in the WMSZ also appear to contain a relatively large component of pure shear and (2), as discussed in Section 5.3, geometric relationships between quartz *c*-axis fabrics and the shape fabric in the WMSZ preclude rotation of lineation into a vertical orientation (Fig. 6d,e). We emphasize that our quartz *c*-axis fabric data demonstrate that the steeply plunging lineation is a true principal stretching direction (Fig. 6c) rather than a finite strain feature produced by combined simple and pure shear deformation bearing no direct relationship to the imposed kinematic framework (Fig. 6e). Consequently, it seems that none of the currently available numerical simulations of transpression zones can fully explain the deformation fabrics observed within the WMSZ.

6.2. Conceptual kinematic model for the WMSZ

Within the WMSZ, we recognize coeval stable segregated domains of simple shear-dominated and pure shear-dominated fabrics (Fig. 7) that accommodate transcurrent and contractional components of deformation respectively. Three key

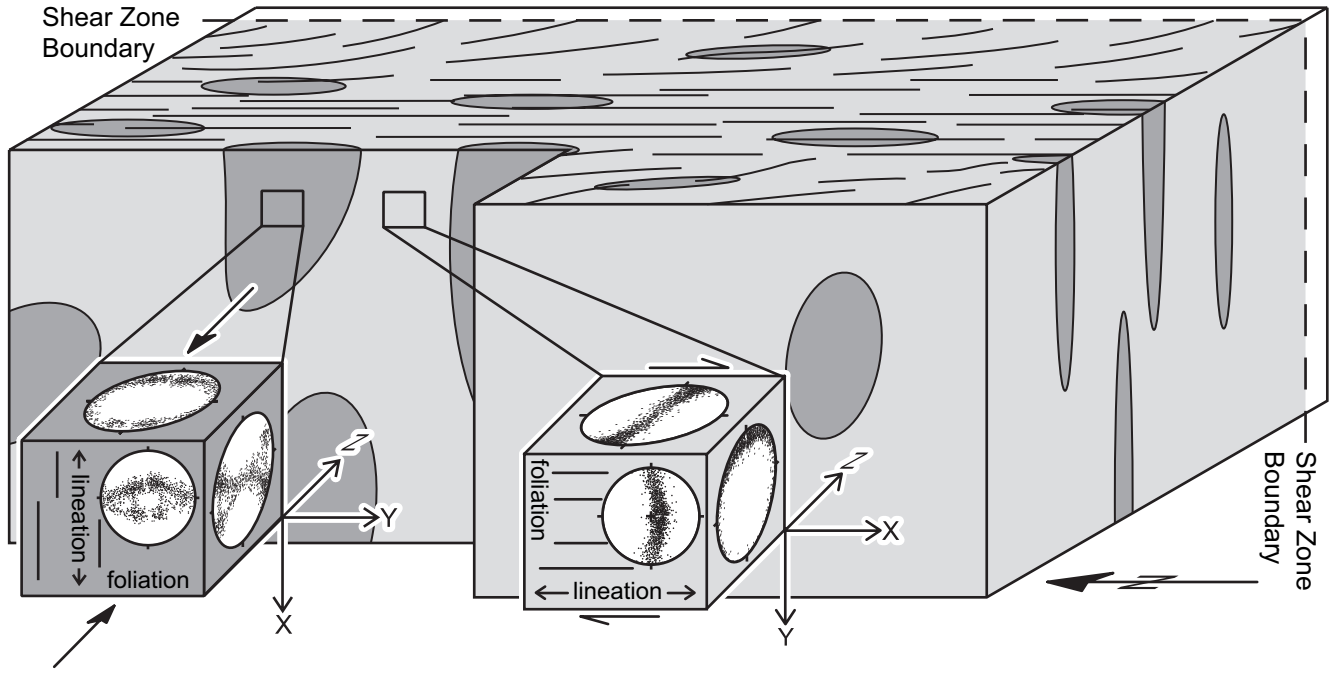

Fig. 7. Conceptual kinematic model for the WMSZ. Dark gray areas represent domains of pure shear-dominated contractional deformation, and light gray areas represent domains of simple shear-dominated transcurrent deformation. The observed quartz *c*-axis fabric patterns are depicted in the small block diagrams from each of the two domains. The idealized foliation orientation is outlined on the top of the large block diagram.

observations can help constrain possible geometries of these domains. First, there is no significant difference in foliation orientation (maximum shortening direction) between simple shear-dominated and pure shear-dominated domains. Second, within the resolution of our transect mapping, pure shear-dominated domains appear to consist of discrete isolated bodies that are volumetrically subordinate to simple shear-dominated domains. Finally, in the pure shear-dominated domains, the maximum finite stretching direction and hence the extrusion direction ranges from subhorizontal to subvertical. Based on these observations and our microstructural and crystallographic fabric data, we propose a conceptual kinematic model for the WMSZ consisting of coeval segregated lozenge-shaped pure shear-dominated domains with variable extrusion directions surrounded by an anastomosing network of simple shear-dominated domains that accommodate the contractional and transcurrent components of deformation respectively (Fig. 7). This overall geometry allows bulk flattening strain across the WMSZ despite the fact that individual domains appear to be characterized by plane strain deformation. Additionally, individual domains within the WMSZ exhibit either a monoclinic or an orthorhombic symmetry, but because the finite stretching directions of the different domains are not at right angles to one another, the zone exhibits a bulk triclinic symmetry. This conceptual model is similar to one proposed by Hudleston, 1999 for maintaining strain compatibility in shear zones, except that in Huddleston's conceptual model the maximum extension direction of the pure shear-dominated domains is parallel to the movement direction of the simple shear component.

Strain compatibility between domains is a potential problem in our conceptual model. However, it is likely easier to maintain strain compatibility between localized segregated kinematic domains than between a homogeneously extruding shear zone and its wall rocks. This is because the local disparities between domains are smaller than the bulk disparity that would be localized along a single contact in a homogeneously extruding zone. Segregated simple shear and pure shear-dominated deformation fabrics within a transpression zone have also been recognized by Goodwin and Williams (1996) who found that compatibility between different domains was accommodated by discrete, lithologically distinct zones of simple shear similar to the stretching faults of Means (1989). If this is the case in the WMSZ, it has not been recognized. However, we propose that stretching faults between kinematic domains are a possibility and that the component of oblique motion recorded in some of the steeply lineated samples may be a manifestation of this.

7. Conclusions and implications

The data presented here demonstrate that strain partitioning between coeval simple shear and pure shear-dominated domains within the transpressional WMSZ has played an important role in the development of the shear zone fabrics. This assertion is based on geometric relationships between quartz *c*-axis fabrics and shape fabrics that show that the maximum principal stretching direction has remained stable with respect to the external kinematic framework imposed upon the sample. That is, there has been little or no abrupt strain-induced transition from subhorizontal to steeply plunging lineations as predicted by numerical simulations of transpression zones. Instead, the steeply plunging lineations within the WMSZ are associated with qualitatively large components of pure shear-dominated deformation, while the shallowly lineated domains are primarily characterized by simple shear-dominated deformation, and, in all cases, the orientation of foliations and lineations in both of these kinematic domains has remained stable. Therefore, we recognize stable discrete coeval segregated kinematic domains of pure shear-dominated and simple shear-dominated deformation within the WMSZ that accommodate the contractional and transcurrent components of transpression respectively, and we propose a geometry wherein the pure shear-dominated domains are lozenge-shaped bodies surrounded by an anastomosing network of simple shear dominated domains.

The partitioning of pure shear and simple shear within the WMSZ into separate discrete kinematic domains could not have been recognized without the quartz *c*-axis fabric data. Because of this we propose that, whenever feasible, quartz crystallographic fabric data should be collected from potential transpression zones in order to determine the extent of strain partitioning that may be taking place within these zones and to test the applicability of numerical simulations involving homogenously distributed pure shear and a finite strain driven change in orientation of the maximum finite stretching direction.

Acknowledgments

W.A.S. gratefully acknowledges grants from Sigma Xi, the University of California White Mountain Research Station (WMRS), and the Virginia Tech David R. Wones Geoscience Scholarship Fund that supported fieldwork associated with this project. We thank Scot Hetzler and Cecil Patrick for their generous support and hospitality during fieldwork and the WMRS administration for their long-term logistical and financial support of our research in the White-Inyo Mountains. John Bartley generously provided a preprint of his paper on dextral off-set across the Owens Valley. Chuck Bailey, Rich Schweickert and Sandra Wyld reviewed an earlier version of this paper. Basil Tikoff also provided helpful comments. David Greene and Laurel Goodwin provided thorough reviews that have greatly improved the quality of the final version of this paper. Bob Holdsworth (editor) was not only very helpful throughout the peer review process, but also managed incredibly quick turn-around times.

References

Bartley, J.M., Glazner, A.F., Coleman, D.S., Kylander-Clark, A.K.C., Friedrich, A.M., in press. Large dextral offset across Owens Valley, California, and its possible relation to tectonic unroofing of the southern Sierra Nevada, in: Till, A.B., Roeske, S.M., Foster, D.A., Sample, J.C. (Eds.),

Exhumation Processes Along Major Continental Strike-slip Fault Systems: Geological Society of America Special Paper.

Berthé, D., Choukroune, P., Gapais, D., 1979. Orthogneiss mylonite and non-coaxial deformation of granites: the example of the South Armorican shear zone. Journal of Structural Geology 1, 31–42.

Bouchez, J.L., Duval, P., 1982. The fabric of polycrystalline ice deformed in simple shear: experiments in torsion, natural deformation and geometrical interpretation. Textures and Microstructures 5, 171–190.

Chetty, T.R.K., Bhaskar Rao, Y.J., 1998. Behavior of stretching lineations in the Salem-Attur shear belt, southern granulite terrane, south India. Journal Geological Society of India 52, 443–448.

Coleman, D.S., Briggs, S., Glazner, A.F., Northrup, C.J., 2003. Timing of plutonism and deformation in the White Mountains of eastern California. Geological Society of America Bulletin 115, 48–57.

Crowder, D.F., Ross, D.C., 1973. Petrography of Some Granitic Bodies in the Northern White Mountains, California-Nevada. In: U.S. Geological Survey Professional Paper. 775.

Crowder, D.F., Sheridan, M.F., 1972. Geologic map of the White Mountain Peak quadrangle Mono County, California. U.S. Geological Survey Map GQ-1012, scale 1. 62,500.

Crowder, D.F., Robinson, P.F., Harris, D.L., 1972. Geologic map of the Benton quadrangle Mono County, California and Esmeralda and Mineral Counties, Nevada. U.S. Geological Survey Map GQ-1013, scale 1. 62,500.

Crowder, D.F., McKee, E.H., Ross, D.C., Krauskopf, K.B., 1973. Granitic rocks of the White Mountains area, California-Nevada: age and regional significance. Geological Society of America Bulletin 84, 285–296.

Czeck, D.M., Hudleston, P.J., 2003. Testing models for obliquely plunging lineations in transpression: a natural example and theoretical discussion. Journal of Structural Geology 25, 959–982.

Dutton, B.J., 1997. Finite strains in transpression zones with no boundary slip. Journal of Structural Geology 19, 1189–1200.

Fates, D.G, 1985. Mesozoic (?) metavolcaniclastic rocks, northern White Mountains, California: structural style, lithology, petrology, depositional setting and paleogeographic significance. M.S. thesis, University of California, Los Angeles.

Flinn, D., 1965. On the symmetry principle and the deformation ellipsoid. Geological Magazine 102, 36–45.

Fossen, H., Tikoff, B., 1993. The deformation matrix for simultaneous simple shearing, pure shearing and volume change, and its application to transpression-transtension tectonics. Journal of Structural Geology 14, 413–422.

Giorgis, S., Tikoff, B., McClelland, W., 2005. Missing Idaho arc: Transpressional modification of the $^{87}Sr/^{86}Sr$ transition on the western edge of the Idaho batholith. Geology, 469–472.

Glazner, A.F., Lee, J., Coleman, D.S., Kylander-Clark, A., Green, D.C., Le, K., 2005. Large Dextral Off-Set across Owens Valley, California from 148 Ma to 1872 A.D. Geological Society of America Penrose Field Forum Guide Book, 35 pp.

Goodwin, L.B., Tikoff, B., 2002. Competency contrast, kinematics, and the development of foliations and lineations in the crust. Journal of Structural Geology 24, 1065–1085.

Goodwin, L.B., Williams, P.F., 1996. Deformation path partitioning within a transpressive shear zone, Marble Cove, Newfoundland. Journal of Structural Geology 18, 975–990.

Green, D.C., Schweickert, R.A., 1995. The Gem Lake shear zone: Cretaceous dextral transpression in the northern Ritter Range pendant, eastern Sierra Nevada, California. Tectonics 14, 945–961.

Hanmer, S., Passchier, C.W., 1991. Shear-sense indicators: a review. Geological Survey of Canada paper 90-17.

Hanson, R.B., 1986. Geology of Mesozoic metavolcanic and metasedimentary rocks, northern White Mountains, California. Ph.D. thesis, University of California, Los Angeles.

Harland, W.B., 1971. Tectonic transpression in Caledonian Spitsbergen. Geological Magazine 108, 27–42.

Heilbronner, R., Tullis, J., 2002. The effect of static annealing on microstructures and crystallographic preferred orientations of quartzites experimentally deformed in axial compression and shear. In: DeMeer, S., Drury, M.R., De Bresser, J.H.P., Pennock, G.M. (Eds.), Deformation Mechanisms, Rheology and Tectonics: Current Status and Future Perspectives. Geological Society, London, Special Publications, vol. 200, pp. 191–218.

Heilbronner, R., Tullis, J., 2006. Evolution of *c*-axis pole figures and grain size during dynamic recrystallization: Results from experimentally sheared quartzite. Journal of Geophysical Research 111, B10202, doi:10.1029/2005JB004194.

Herwegh, M., Handy, M.R., 1996. The evolution of high temperature mylonitic microfabrics: evidence for simple shearing of a quartz analogue (norcamphor). Journal of Structural Geology 18, 689–710.

Herwegh, M., Handy, M.R., Heilbronner, R., 1997. Temperature- and strain rate-dependent microfabric evolution in monomineralic mylonite: evidence from in-situ deformation of norcamphor. Tectonophysics 280, 83–106.

Hirth, G., Tullis, J., 1992. Dislocation creep regimes in quartz aggregates. Journal of Structural Geology 14, 145–160.

Holdsworth, R.E., Strachran, R.A., Dewey, J.F. (Eds.), 1998. Continental Transpressional and Transtensional Tectonics. Geological Society of London Special Publication, 135.

Hudleston, P.J., 1999. Strain compatibility in shear zones: is there a problem? Journal of Structural Geology 21. 932–932.

Jiang, D., 1994a. Vorticity determination, distribution, partitioning and the heterogeneity and non-steadiness of natural deformations. Journal of Structural Geology 16, 121–130.

Jiang, D., 1994b. Flow variation in layered rocks subjected to bulk flow of various kinematic vorticities: theory and geological implications. Journal of Structural Geology 16, 1159–1172.

Jiang, D., Williams, P.F., 1998. High-strain zones: a unified model. Journal of Structural Geology 20, 1105–1120.

Jessell, M., Lister, G.S., 1990. A simulation of the temperature dependence of quartz fabrics. In: Knipe, R.J., Rutter, E.H. (Eds.), Deformation Mechanisms, Rheology and Tectonics. Geological Society, London, Special Publications, vol. 54, pp. 353–362.

Jones, R.R., Holdsworth, R.E., 1998. Oblique simple shear in transpression zones. In: Holdsworth, R.E., Strachran, R.A., Dewey, J.F. (Eds.), Continental Transpressional and Transtensional Tectonics. Geological Society, London, Special Publications, vol. 135, pp. 35–40.

Jones, R.R., Tanner, P.W.G., 1995. Strain partitioning in transpression zones. Journal of Structural Geology 17, 793–802.

Jones, R.R., Holdsworth, R.E., Bailey, W., 1997. Lateral extrusion in transpression zones: the importance of boundary conditions. Journal of Structural Geology 19, 1201–1217.

Jones, R.R., Holdsworth, R.E., Clegg, P., McCaffrey, K., Tavarnelli, E., 2004. Inclined transpression. Journal of Structural Geology 26, 1531–1548.

Kylander-Clark, A.R.C., Coleman, D.S., Glazner, A.F., Bartley, J.M., 2005. Evidence for 65 km of Dextral Slip Across Owens Valley, California, since 83 Ma. Geological Society of America Bulletin 117, 962–968.

Law, R.D., 1986. Relationships between strain and quartz crystallographic fabrics in the Roche Maurice quartzites of Plougastel, western Brittany. Journal of Structural Geology 8, 493–515.

Law, R.D., 1987. Heterogeneous deformation and quartz crystallographic fabric transitions: natural examples from the Moine thrust zone at the stack of Glencoul, northern Assynt. Journal of Structural Geology 9, 819–833.

Law, R.D., 1990. Crystallographic fabrics: a selective review of their applications to research in structural geology. In: Knipe, R.J., Rutter, E.H. (Eds.), Deformation Mechanisms, Rheology and Tectonics. Geological Society, London, Special Publications, vol. 54, pp. 335–352.

Lee, J., Spencer, J., Owen, L., 2001. Holocene slip rates along the Owens Valley fault, California: Implications for the recent evolution of the eastern California shear zone. Geology 29, 819–822.

Lin, S., Jiang, D., Williams, P.F., 1992. The origin of ridge-in-groove slickenside striae and associated steps in an S-C mylonite. Journal of Structural Geology 14, 315–321.

Lin, S., Jiang, D., Williams, P.F., 1998. Transpression (or transtension) zones of triclinic symmetry: natural example and theoretical modeling. In: Holdsworth, R.E., Strachran, R.A., Dewey, J.F. (Eds.), Continental Transpressional and Transtensional Tectonics. Geological Society, London, Special Publications, vol. 135, pp. 41–57.

Lister, G.S., 1977. Crossed-girdle *c*-axis fabrics in quartzites plastically deformed by plane strain and progressive simple shear. Tectonophysics 39, 51–54.

Lister, G.S., Hobbs, B.E., 1980. The simulation of fabric development during plastic deformation and its application to quartzite: the influence of deformation history. Journal of Structural Geology 2, 355–370.

Lister, G.S., Snoke, A.W., 1984. S-C mylonites. Journal of Structural Geology 6, 617–638.

Lister, G.S., Williams, P.F., 1983. The partitioning of deformation in flowing rock masses. Tectonophysics 92, 1–33.

Lister, G.S., Patterson, M.S., Hobbs, B.E., 1978. The simulation of fabric development during plastic deformation and its application to quartzite: the model. Tectonophysics 45, 107–158.

McKee, E.H., Conrad, J.E., 1996. A tale of 10 plutons, revisited: Age of granitic rocks in the White Mountains, California and Nevada. Geological Society of America Bulletin 108, 1515–1527.

Means, W.D., 1989. Stretching faults. Geology 17, 893–896.

Morgan, S.S., Law, R.D., 1998. An overview of Paleozoic and Mesozoic structures developed in the central White-Inyo Range, eastern California. International Geology Review 40, 245–256.

Passchier, C.W., 1988. Analysis of deformation paths in shear zones. Geologisches Rundschau 77, 309–318.

Price, J.P., 1985. Preferred orientations in quartzites. In: Wenk, H.R. (Ed.), Preferred Orientations in Deformation Metals and Rocks: An Introduction to Modern Texture Analysis. Academic Press, Orlando, pp. 385–406.

Ramsay, J.G., Graham, R.H., 1970. Strain variation in shear belts. Canadian Journal of Earth Sciences 7, 786–813.

Robin, P.Y., Cruden, A.R., 1994. Strain and vorticity patterns in ideally ductile transpression zones. Journal of Structural Geology 16, 447–466.

Sanderson, D.J., Marchini, W.R.D., 1984. Transpression. Journal of Structural Geology 6, 449–458.

Schmid, S.M., Casey, M., 1986. Complete fabric analysis of some commonly observed quartz *c*-axis patterns. American Geophysical Union Geophysical Monograph 36, 263–286.

Simpson, C., De Paor, D.G., 1993. Strain and kinematic analysis in general shear zones. Journal of Structural Geology 15, 1–20.

Simpson, C., De Paor, D.G., 1997. Practical analysis of general shear zones using the porphyroclast hyperbolic distribution method: an example from the Scandinavian Caledonides. In: Sengupta, S. (Ed.), Evolution of Geological Structures in Micro- to Macro-scales. Chapman and Hall, London, pp. 169–184.

Stern, T.W., Bateman, P.C., Morgan, B.A., Newell, M.F., Peck, D.L., 1981. Isotopic U-Pb ages of zircons from the granitoids of the central Sierra Nevada, California. U.S. Geological Survey Professional Paper 1185.

Stevens, C.H., Stone, P., 2002. Correlation of Permian and Triassic deformations in the western Great Basin and eastern Sierra Nevada: evidence from the northern Inyo Mountains near Tinemaha Reservoir, east-central California. Geological Society of America Bulletin 114, 1210–1221.

Stevens, C.H., Stone, P., Dunne, G.C., Greene, D.C., Walker, J.D., Swanson, B.J., 1997. Paleozoic and Mesozoic evolution of east-central California. International Geology Review 39, 788–829.

Stevens, C.H., Stone, P., Greene, D.C., 2003. Correlation of Permian and Triassic deformations in the western Great Basin and eastern Sierra Nevada: evidence from the northern Inyo Mountains near Tinemaha Reservoir, east-central California: Reply. Geological Society of America Bulletin 115, 1309–1311.

Stewart, J.H., 1980. Regional tilt patterns of late Cenozoic Basin-Range fault blocks, western United States. Geological Society of America Bulletin 91, 460–464.

Stockli, D.F., Farley, K.A., Dumitru, T.A., 2000. Calibration of the apatite (U-Th)/He thermochronometer on an exhumed fault block, White Mountains, California. Geology 28, 983–986.

Stockli, D.F., Dumitru, T.A., McWilliams, M.O., Farley, K.A., 2003. Cenozoic tectonic evolution of the White Mountains, California and Nevada. Geological Society of America Bulletin 115, 788–816.

Sullivan, W.A., 2003. Geometry, kinematics and age of the northern half of the White Mountain shear zone, California and Nevada. M.S. thesis, Virginia Polytechnic Institute and State University.

Takeshita, T., Wenk, H.R., Lebensohn, R., 1999. Development of preferred orientation and microstructure in sheared quartzite: comparison of natural data and simulated results. Tectonophysics 312, 133–155.

Tikoff, B., Greene, D.C., 1997. Stretching lineations in transpressional shear zones: an example from the Sierra Nevada batholith, California. Journal of Structural Geology 19, 29–39.

Tikoff, B., Saint Blanquat, M., 1997. Transpressional shearing and strike-slip partitioning in the late Cretaceous Sierra Nevada magmatic arc, California. Tectonics 16, 442–459.

Tikoff, B., Teyssier, C., 1994. Strain modeling of displacement field partitioning in transpressional orogens. Journal of Structural Geology 16, 1575–1588.

Tullis, J., 1977. Preferred orientation of quartz produced by slip during plane strain. Tectonophysics 39, 87–102.

United States Geological Survey, California Division of Mines and Geology, 1966. Geologic Map of California. USGS Map I-512.

Vines, J.A., 1999. Emplacement of the Santa Rita Flat pluton and kinematic analysis of cross cutting shear zones, eastern California. M.S. thesis, Virginia Polytechnic Institute and State University.

Wallis, S.R., 1992. Vorticity analysis in a metachert from the Sanbagawa Belt, SW Japan. Journal of Structural Geology 14, 271–280.

Wallis, S.R., 1995. Vorticity analysis and recognition of ductile extension in the Sanbagawa belt, SW Japan. Journal of Structural Geology 17, 1077–1093.

Wenk, H.R., Canova, G., Molinari, A., Kocks, U.F., 1989. Visco-elastic modeling of texture development in quartzite. Journal of Geophysical Research 94, 17895–17906.